Australian Earthquake Engineering Society 2019 Conference, 29 Nov-1 Dec, Newcastle, NSW

The 2018 Lake Muir earthquake sequence, southwest Western Australia: rethinking the relationship between magnitude and surface rupture length for Australian stable continental region earthquakes

Dan J. Clark[1], Trevor I. Allen[1], Sarah Brennand[1], Gregory Brenn[1], Matthew C. Garthwaite[1], Sean Standen[2]

[1] Positioning and Community Safety Division, Geoscience Australia, GPO Box 378 Canberra ACT, Australia
[2] The University of Western Australia, 35 Stirling Hwy, Crawley, Western Australia, Australia

Email: dan.clark@ga.gov.au

Abstract

Modern geodetic and seismic monitoring tools are enabling the study of moderate-sized earthquake sequences in unprecedented detail. Discrepancies are apparent between the surface deformation envelopes 'detectable' using these tools, and 'visible' to traditional ground-based methods of observation. As an example, we compare the detectible and visible surface deformation caused by a sequence of earthquakes near Lake Muir in southwest Western Australia in 2018. A shallow M_W 5.3 earthquake on the 16th of September 2018 was followed on the 8th of November 2018 by a M_W 5.2 event in the same region. Focal mechanisms for the events suggest reverse and strike-slip rupture, respectively. Interferometric Synthetic Aperture Radar (InSAR) analysis of the events suggests that the ruptures are in part spatially coincident and deformed the Earth's surface over ~ 12 km in an east-west direction and ~ 8 km in a north-south direction. Field mapping, guided by the InSAR results, reveals that the first event produced an approximately 3 km long and up to 0.5 m high west-facing surface rupture, consistent with slip on a moderately east-dipping fault. No surface deformation unique to the second event was identifiable on the ground. New rupture length versus magnitude scaling relationships developed for non-extended cratonic regions as part of this study allow for the distinction between 'visible' surface rupture lengths (VSRL) from field-mapping and 'detectable' surface rupture lengths (DSRL) from remote sensing techniques such as InSAR, and suggest longer ruptures for a given magnitude than implied by commonly used scaling relationships.

Keywords: earthquake recurrence, Precambrian Craton, earthquake, paleoseismology

INTRODUCTION

The Lake Muir earthquake sequence

The M_L 5.7 (M_W 5.3) Lake Muir earthquake occurred at 04:56:24 (UTC) on 16th September 2018 in a rural area of southwest Western Australia (**Figure 1**). Approximately 20 km from the epicentre, relatively modest Modified Mercalli Intensity (MMI) values of VI were reported (Allen *et al.*, 2019a; Allen *et al.*, 2019b). With the exception of one unoccupied dwelling in the immediate epicentral area, which was extensively damaged, only minor damage and no injuries were reported. The event was widely felt throughout the Perth Basin, including the Perth metropolitan region, over 300 km away. Focal mechanisms suggest a reverse faulting mechanism, with a minor dextral transcurrent component, and moderately east and northwest dipping nodal planes (https://earthquake.usgs.gov/earthquakes/eventpage/us2000hfcw). Geoscience Australia recorded a magnitude M_L 3.4 foreshock three days prior to the main shock. A protracted aftershock sequence, comprising hundreds of located events, was punctuated by a M_L 4.7 event on 12th October at 16:31:30 (UTC). Almost two months after the 16th September M_W 5.3 event, a M_L 5.4 (M_W 5.2) event occurred on the 8th November at 21:07:01 (UTC). Within the error estimates of the hypocentral determinations, this event was co-located with the 16th September event. The focal mechanisms calculated for the November event indicate predominantly dextral strike-slip faulting, with steeply northwest and southwest dipping nodal planes. The percentage double-couple from the USGS W-phase moment tensor solution is 31% (https://earthquake.usgs.gov/earthquakes/eventpage/us1000hpej). This event was felt much more strongly and widely than the slightly larger first event, with MMI of VII to VIII being recorded close to the epicentre.

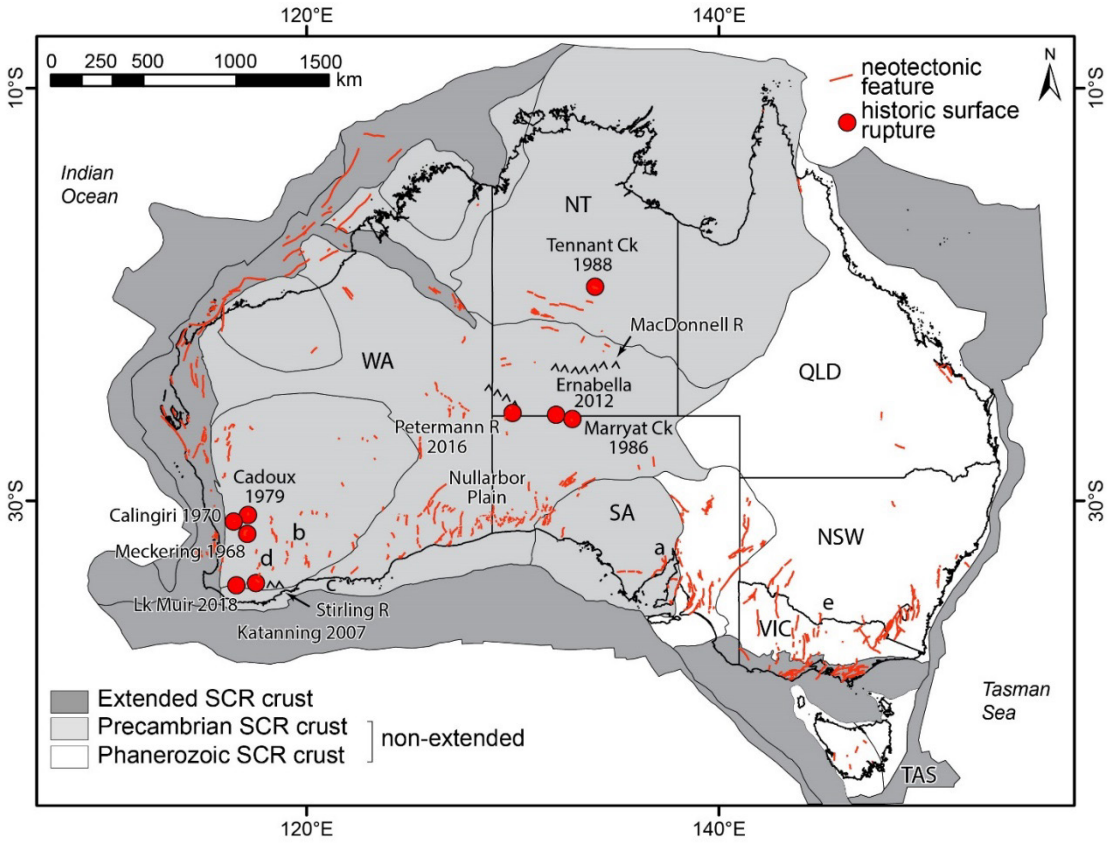

Figure 1: Neotectonic features (red lines) from the Australian Neotectonic Features Database (Clark, 2012; Clark *et al.*, 2012). Historical surface ruptures shown as red dots labelled with the year of the event. Base map shows neotectonic superdomains (after Leonard *et al.*, 2014), and the outlines of Australian States and Territories. Note all historical surface ruptures have occurred in Precambrian stable continental region (SCR, Johnston *et al.*, 1994) crust.

Geological and seismo-tectonic context

The Lake Muir region lies near to the southern boundary of a broad band of relatively high seismicity crossing the southwest corner of Western Australia known as the Southwest Seismic Zone (SWSZ, Doyle, 1971), which is one of the most seismically active regions in Australia (e.g. Leonard, 2008; Allen *et al.*, 2018). Earthquake activity in the SWSZ appears to have increased significantly since the 1940s (Leonard, 2008), and it has generated five of the nine known Australian historic surface ruptures (**Table 1**). In addition to large shallow events and scattered smaller events, the SWSZ has produced several dozen earthquake swarms in the last 40 years, including the Burakin swarm of 2001-2002 during which ~18,000 events (including three above M_L 5.0) were recorded in a period of only a few months (Leonard, 2002; Allen *et al.*, 2006; Dent, 2016). While most swarm centres occur within the SWSZ, they also have a broader distribution across the southwest of Western Australia (Dent, 2016), a pattern that is similar to fault scarps relating to pre-historic events (Clark, 2010; Clark *et al.*, 2012) (**Figure 1**). The relatively uniform spatial distribution of north-trending reverse-fault scarps is consistent with scarp formation under conditions imposed by the contemporary east-west oriented compressive crustal stress regime (e.g. Rajabi *et al.*, 2017), and suggests that strain is uniformly distributed over the Yilgarn Craton over the timescale recorded in the land surface (*ca.* 100 kyr or more) (Leonard & Clark, 2011).

Excluding the November M_W 5.2 event, for which a unique surface rupture could not be mapped in the field (see next section), the September M_W 5.3 Lake Muir earthquake was the ninth event documented to have produced surface rupture in Australia in historical times (**Figure 1, Table 1**). These ruptures are located exclusively in the Precambrian stable continental region (SCR) crust of central and western Australia (**Figure 1**), and none could have been identified and mapped using topographic signature prior to the respective historical events (**Table 1**). Moreover, Crone et al. (1997) excavated trenches across the 1986 Marryat Creek and 1988 Tennant Creek ruptures and found that while each rupture in part exploited pre-existing bedrock faults, there was no unequivocal stratigraphic or structural evidence to suggest a penultimate event in the preceding 50-100 kyr or more. A similar conclusion was made on the basis of trenching investigations of the 1968 Meckering surface rupture (see Clark & Edwards, 2018, and references therein). For the purposes of probabilistic seismic hazard assessment, these earthquakes might be considered as 'one-off' events.

Table 1: Historical earthquake events known to have produced surface rupture in Australia (expanded after Clark *et al.*, 2014). * The Tennant Creek surface rupture was produced by three events in a 12 hr period (Bowman, 1992). # Values in brackets reflect the surface rupture length estimated from InSAR data.

Event	Year	Magnitude (Mw)	Mapped surface rupture length (km)#	Maximum vertical displacement (m)	Reference
Meckering, WA	1968	6.58	37	2.5	Gordon & Lewis (1980); Clark & Edwards (2018)
Calingiri, WA	1970	5.46	3.3	0.4	Gordon & Lewis (1980)
Cadoux, WA	1979	6.13	14	1.4	Lewis *et al.* (1981)
Marryat Creek, SA	1986	5.74	13	0.9	Machette *et al.* (1993)
Tennant Creek, NT*	1988	6.76	36	1.8	Crone e*t al.* (1992; 1997)
Katanning, WA	2007	4.73	0.2 (1.26)	0.1	Dawson *et al.* (2008)
Ernabella, SA	2012	5.37	1.5	0.5	Clark *et al.* (2014)
Petermann Ranges, NT	2016	6.10	15 (20)	1.0	King *et al.* (2018); Polcari et al. (2018); Wang et al. (2019)
Lake Muir, WA	2018	5.30	3.2 (7)	0.4	this article

COMPARISON OF FIELD-BASED AND REMOTE OBSERVATIONS OF THE LAKE MUIR EARTHQUAKE SEQUENCE

Initial reports from local residents following the September earthquake indicated the presence of west-facing fault scarps intersecting several farm tracks (e.g., **Figure 2a**), loss of tension in an east-west running fence line (GDA94/MGA50, 479590 mE, 6192140 mN), and cracking in farm dam walls related to lateral spreading (**Figure 2b**). Field investigation demonstrated that the track intersections could be linked to form an approximately 3 km-long, concave-to-the-east, west-facing crescentic scarp (**Figure 3**). In detail, the scarp comprises a series of left and right stepping *en echelon* segments 100 – 200 m long. In the central 2 km of the scarp, each segment is associated with up to 20 – 40 cm of vertical displacement (**Figure 2c, 2d**). A hand trench excavated near to the centre of the scarp revealed a 30° east-dipping fault tip (Clark *et al.*, 2019). No surface rupture unique to the November earthquake was observed.

The wrapped InSAR interferogram for the September event shows an extent of surface deformation ~ 12 km in an east-west direction and ~ 8 km in a north-south direction (**Figure 3a**). A linear surface deformation front relating to the rupture can be traced for approximately 5 km. The central ~3 km corresponds to the fault scarp mapped on the ground. The rupture terminates at northern and southern ends against highly oblique structures which coincide with aeromagnetic lineaments (Clark *et al.*, 2019). The unwrapped interferogram (similar to a DEM, **Figure 3b**) shows a broad shallow lobe of uplift that extends from the west to the surface scarp. From the east, a broad shallow lobe of land-surface depression transitions to a tight (~1.5 km wide) band of land-surface uplift. Note that the area of maximum uplift peaks to the east of the scarp, suggesting that vertical displacement measurements at the scarp face should be treated as minimum estimates (cf. Clark *et al.*, 2019; Gold *et al.*, 2019). The images lose coherence in the 200 – 300 m east of the scarp, and in proximity to Lake Noobijup. Coherence is also partly lost beneath an approximately 2 km wide (N-S) easterly trending band of pine forest (see **Figures 3a** for location).

The InSAR images for the November event (**Figures 3c & 3d**) exhibit the classic quadrupole pattern of an almost pure strike-slip rupture, and are consistent with a maximum of ~5 – 8 cm of right-lateral deformation having occurred at the surface relating to rupture of a northeast-trending, steeply northwest dipping fault. This contrasts with the focal mechanism for the event, which suggests an oblique compressive rake. Although the deformation pattern shows a sharp linear discontinuity for ~ 1 km either side of the intersection of the November failure plane with the September rupture plane, simple forward modelling using a finite rectangular elastic dislocation model (Okada, 1985) suggests that a discrete surface rupture may not have been produced (i.e., the rupture tip remained shallowly buried), consistent with the field observations.

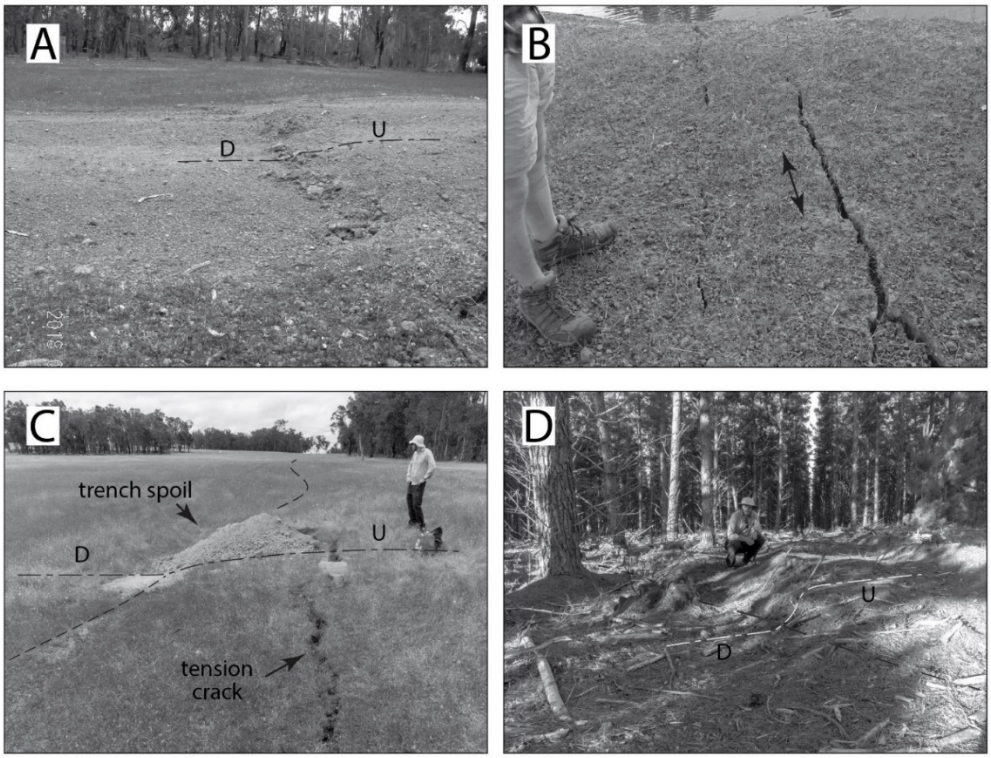

Figure 2: Photographs of the surface rupture: (a) 13 cm high scarp crossing farm track. Photo taken by Roger Hearn on 27/09/2018. Looking north (479101 mE, 6190727 mN); (b) east-trending tension fissures relating to lateral spread into a farm dam (479588 mE, 6192126 mN); (c) 40 cm high scarp and hanging wall tension fissure at the hand trench location (see Clark *et al.*, 2019). Looking north (479285 mE, 6191496 mN); (d) 40 cm high scarp in pine plantation. Looking northeast (479112 mE, 6190422 mN). GD94/MGA50.

RELATIONSHIP BETWEEN MOMENT MAGNITUDE AND SURFACE RUPTURE LENGTH AMONGST AUSTRALIAN CRATONIC EARTHQUAKES

Clark *et al.* (2014) provided scaling relationships between surface rupture-length and moment magnitude for reverse-faulting earthquakes occurring in Australian non-extended cratonic settings. Their relationships demonstrate that in this tectonic setting, earthquakes tend to produce longer earthquake ruptures than may be expected when compared to commonly-used rupture-scaling relationships (e.g. Wells & Coppersmith, 1994; Leonard, 2014). It is hypothesised that shallow crustal detachments in these regions (Dentith *et al.*, 2000; Drummond *et al.*, 2000) or, alternatively, large shallowly dipping thrust faults (Goleby *et al.*, 1989; Camacho *et al.*, 1995; Korsch *et al.*, 1998) combined with high near-surface stresses (Denham *et al.*, 1980; Denham *et al.*, 1987) may favour the occurrence of earthquakes at shallow depths. This suggests that relatively narrow fault widths are available for seismogenic rupture, likely leading to large rupture length-to-width aspect ratios for larger-magnitude earthquakes. Since the Clark *et al.* (2014) relationship was published, the Australian continent has experienced two further surface-rupturing earthquakes with the occurrence of the 2016 Petermann Ranges and 2018 Lake Muir events (see **Table 1**). Including these new data, the Clark *et al.* (2014) scaling relationships are reviewed and updated.

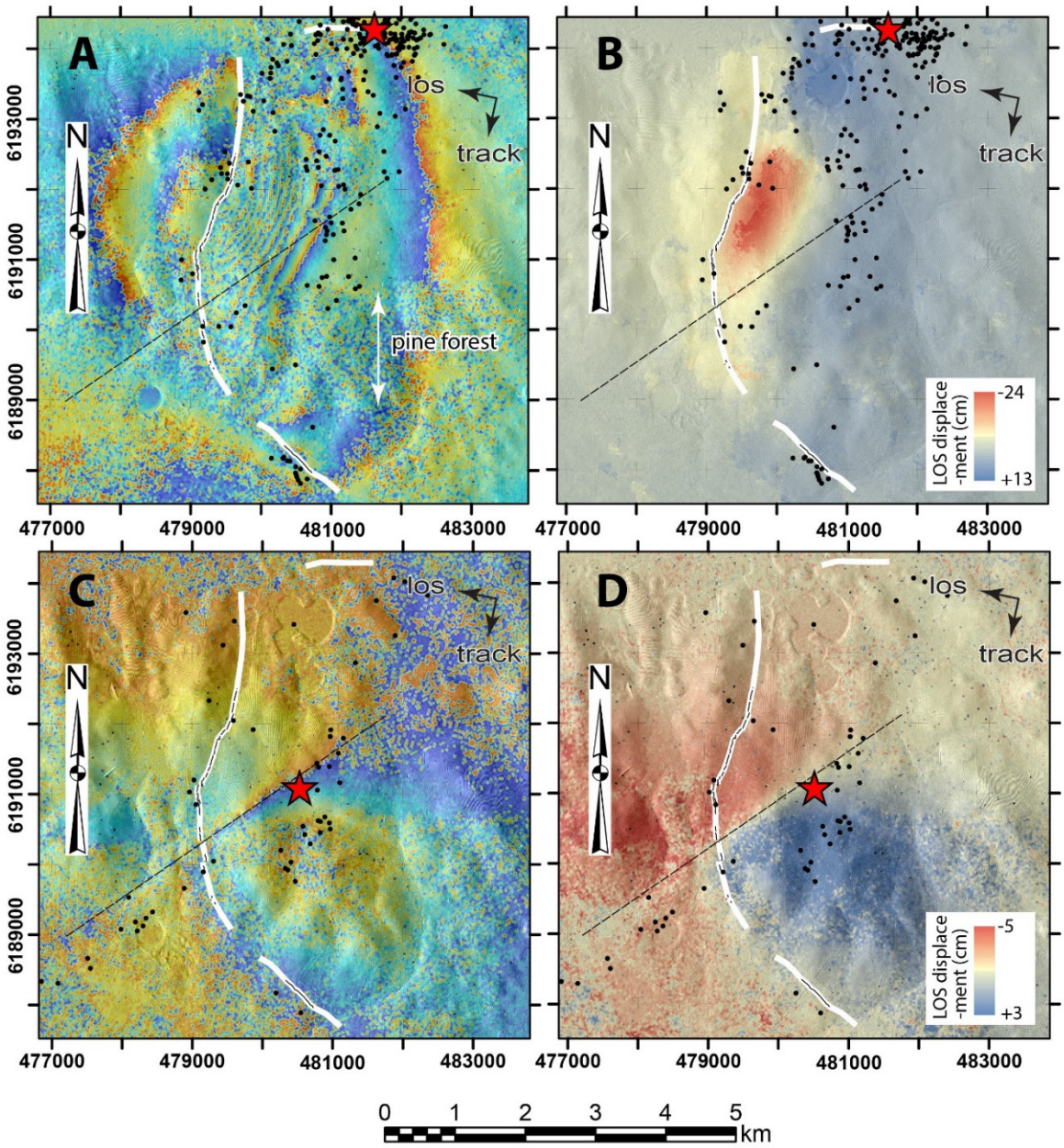

Figure 3: Phase images and images of the unwrapped InSAR line of sight (LOS) displacement field for the (a) & (b) September M_W5.3 and (c) & (d) November M_W5.2 events. The location of the surface rupture relating to the September event is shown as a white line, with a black dashed line showing where the scarp was observed in the field. The surface deformation front relating to the November event is shown as a dashed black line. Seismicity before and after the November event is shown as black dots on parts (a) & (b) and (c) & (d), respectively. The main shocks are shown as red stars. Each fringe in (a) and (c) represents 2.8 cm of LOS range change. Note several unwrapping errors are evident as regions bound by a step jump at the northern and southern end of the scarp in part (b).

With the availability of high-resolution InSAR observations, the extent of earthquake surface deformation can be more readily identified and mapped (e.g. **Figure 3**). Differences between the total "visible" surface rupture lengths (*VSRL*) from field-mapping and "detectable" surface rupture lengths (*DSRL*) from InSAR observations are evident, with the latter observations being longer where these observations are available (**Table 1**). Consequently, regressions are undertaken between: 1) *VSRL* and M_W, and; 2) *DSRL* and M_W. The regression takes the following form:

$$SRL = a + b \times M_W \quad (1)$$

where *SRL* is the generic term given to either *VSRL* or *DSRL* and *a* and *b* are coefficients to be determined through regression (**Table 2**). When *DSRL* from InSAR observations is unavailable, the *DSRL* value is assumed to be equivalent to *VSRL*. It is recognised that this may yield an underestimate of the total rupture length, *DSRL*.

Figure 4a and 4b shows the least squares relationships relative to other rupture-length scaling relationships used for non-extended cratonic regions. In general, the updated regressions suggest longer surface ruptures for a given earthquake magnitude, with likely convergence of *DSRL* length-magnitude relations with those estimated by Clark *et al.* (2014) taking place near M_W 7.0.

Because of the likely biases imposed from assuming *DSRL* = *VSRL* for those ruptures that do not have available InSAR observations, a relationship between the ratio of *VSRL* – *DSRL* and *VSRL* is constructed using limited data from three earthquakes where independent *VSRL* and *DSRL* estimates exist (**Figure 4c**). It is assumed that earthquakes with decreasing magnitudes and increasing depth will be expressed at the Earth's surface with decreasing *VSRL* discoverability. The ratio of *VSRL* and *DSRL* could thus be used as a correction factor that could be applied to *VSRL* observations where independent estimates of *DSRL* do not exist. A literature search, which included international studies, did not yield any additional data that could be added to the available dataset, particularly for reverse-mechanism ruptures in non-extended cratonic regions. The proposed *VSRL* to *DSRL* correction factor, γ, can be calculated following:

$$\gamma = \min(\delta, 1.0) \quad (2a)$$

where:

$$\log_{10} \delta = 0.362 \times \log_{10} VSRL - 0.540 \quad (2b)$$

The corrected detectable surface rupture length (*DSRL'*), can thus be determined following:

$$DSRL' = VSRL / \gamma \quad (2c)$$

Supplementing the values of *DSRL'* for events where *DSRL* is not directly measured, revised rupture-scaling relationships between *DSRL'* and M_W can be developed (**Figure 4d; Table 2**). These revised scaling relationships demonstrate longer rupture lengths for smaller-magnitude earthquakes with lower standard deviation of the residuals (**Table 2**).

The authors recognise that these relationships are highly conjectural and are based on very limited data. Consequently, the authors invite additional researchers to augment these data to fully scrutinise the legitimacy of the relationships. Nevertheless, these fault-scaling approaches may have future utility in improving the characterisation of neotectonic fault scarps and their potential characteristic magnitudes. Should these approaches be refined, they may lead to a decrease in characteristic magnitudes on neotectonic fault scarps in non-extended cratonic regions, such as central and western Australia.

Table 2. Coefficients between *SRL* (*VSRL* or *DSRL* in km) and M_W for substitution into Equation 1. * the regression type used is either least squares (LSQ) or orthogonal distance (ODR) regression, respectively.

Regression*	*a*	*a (std err)*	*b*	*b (std err)*	Std
VSRL (LSQ)	-5.38	0.788	1.064	0.135	0.250
VSRL (ODR)	-5.76	0.815	1.130	0.140	0.169
DSRL (LSQ)	-3.58	0.733	0.777	0.126	0.233
DSRL (ODR)	-3.91	0.753	0.833	0.129	0.181
DSRL' (LSQ)	-2.97	0.480	0.693	0.082	0.152
DSRL' (ODR)	-3.10	0.485	0.716	0.083	0.125

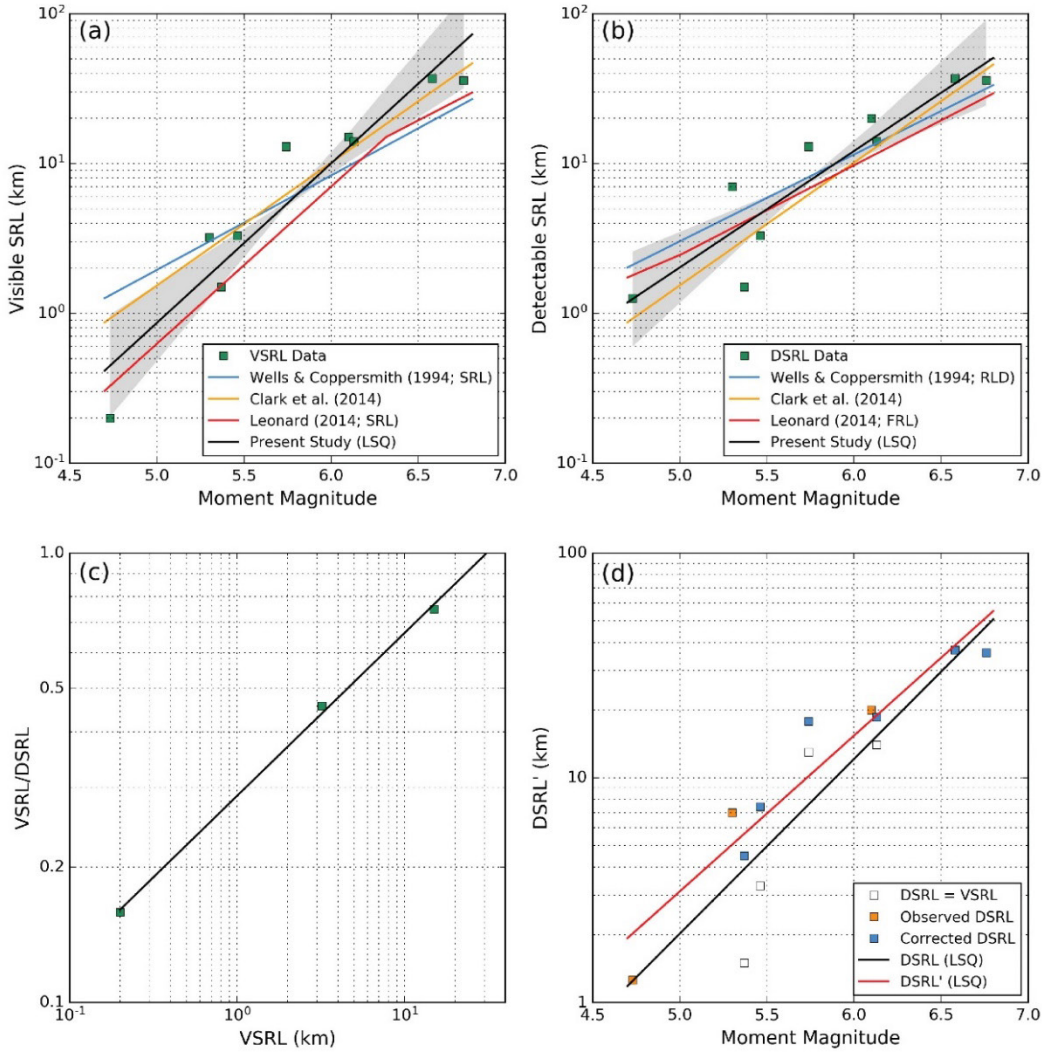

Figure 4: The least squares relationships for (a) VSRL and (b) DSRL relative to other magnitude-rupture length scaling relationships, including Wells and Coppersmith (1994; surface rupture length and sub-surface rupture length, respectively), Clark et al (2014b) and Leonard (2014; surface rupture length and fault rupture length for SCR dip-slip events, respectively). Grey areas stretch between the upper and lower confidence bounds of our LSQ regression (at 95% confidence). (c) The ratio of VSRL and DSRL plotted against VSRL used to determine the postulated correction factor used to calculate DSRL' as shown in Equation 2. (d) Corrected DSRL' values based on adjustment factors in Equation 2. Note, data points where DSRL = VSRL are plotted for reference but are not used to determine the magnitude scaling coefficients in **Table 2**.

DISCUSSION

Earthquake "recurrence" on Australian seismogenic faults

Conceptually, for the purposes of probabilistic seismic hazard assessment, a *fault source* is a seismogenic fault that has produced earthquakes in the past, and can be expected to continue doing so (Musson, 2012). A preponderance of 'one-off' events in Australian Precambrian SCR crust suggests caution in applying a traditional elastic strain accumulation model (cf. Braun *et al.*, 2009; Clark, 2010). Indeed, over the last few decades, permanent and campaign GPS studies have failed to detect a tectonic deformation signal from which a strain budget could be calculated across all of Australia (e.g. Tregoning, 2003). Similar studies have used these observations, amongst others (e.g. Calais *et al.*, 2005), to propose that one-off events and clusters of large events either deplete long-lived pools of 'fossil' lithospheric stress (Calais *et al.*, 2016; Liu & Stein, 2016) and/or that there is an orders of magnitude difference in the timescales of elastic strain accumulation and seismogenic

strain release (e.g. Clark *et al.*, 2015; Craig *et al.*, 2016). By virtue of the scarcity of data with which to validate such a model, the underpinning assumption that a 'long-term slip rate' is a meaningful concept in an intraplate setting, as per the prevailing plate margin paradigm, remains to be fully tested. Indications are that the concept may be useful in the Phanerozoic stable continental region (SCR) crust of eastern Australia (**Figure 1**), where faults with up to a few hundreds of metres of neotectonic slip occur (cf. Clark *et al.*, 2015; Clark *et al.*, 2017). However, it is not so certain whether assigning a long-term slip rate is meaningful for structures within Precambrian SCR crust (e.g. Calais *et al.*, 2016). In the general absence of evidence for recurrence of large events, building relations for fault displacement hazard using rupture traces from cratonic Australia is fraught (cf. Boncio *et al.*, 2018).

New insight into non-extended SCR rupture characteristics

As was the case with the 2016 Petermann Ranges earthquake rupture (King *et al.*, 2018; Polcari *et al.*, 2018; Gold *et al.*, 2019; Wang *et al.*, 2019), the Lake Muir September event surface rupture was longer than might have been expected from scaling relationships between magnitude and surface rupture length (e.g. Wells & Coppersmith, 1994; Clark *et al.*, 2014; Leonard, 2014). New relationships developed as part of this study (**Figure 4**, see also Clark et al. (2019)) allow for the distinction between "visible" surface rupture lengths (*VSRL*) from field-mapping, and "detectable" surface rupture lengths (*DSRL*) from increasingly more readily available InSAR data that more closely define the complete rupture extent . Relative to the scaling relationships introduced by Clark et al. (2014) (equivalent to the VSRL relationships presented here), the updated relationships include more data and yield lower uncertainties, particularly when the *DSRL* is used. In general, the *DSRL* scaling relationships will yield longer ruptures for a given event magnitude, converging with the Clark et al. (2014) scaling relationships near M_W 7.0. Users should exercise caution extending these relationships to lower magnitudes where the intersection of the rupture plane with the surface becomes less likely. Nevertheless, the relatively large rupture lengths observed for moderate-to-large earthquakes in non-extended Australian cratonic crust challenges notions that SCR earthquakes should yield higher stress drops (e.g., Allmann & Shearer, 2009), with smaller rupture areas (e.g., Brune, 1970). Conservation of high stress drop for SCR events, commensurate with Allmann and Shearer (2009), would require narrow down-dip rupture widths (to minimise area) that yield large aspect ratios. The surface displacement field revealed in the InSAR suggests that the rupture width is < 2.0 km, suggesting non-uniform scaling between rupture length and width. Systematic analysis of stress drop for recent moderate-to-large ($M_W \geq 5.0$) Australian earthquakes should be undertaken to test the nature of stress drop relative to surface rupture to provide further constraint on the expected rupture dimensions of SCR earthquakes in Australia.

CONCLUSIONS

A shallow M_W 5.3 earthquake near Lake Muir in southwest Western Australia on the 16th of September 2018 was followed on the 8th of November by a co-located M_W 5.2 event. Focal mechanisms produced for the events suggest reverse and strike-slip rupture, respectively. Recent improvements in the coverage and frequency of synthetic aperture radar data over Australia with the Sentinel-1 satellite constellation has allowed for the timely mapping of the surface deformation fields relating to both earthquakes in unprecedented detail. Field mapping, guided by the InSAR data, reveal that the first event produced an approximately 3 km-long and up to 0.4-0.6 m high west-facing surface rupture, consistent with slip on a moderately east-dipping fault. Interpretation of InSAR data shows that the surface scarp relates to a sub-surface rupture ~5 km long, bound at its north and southern extremities by strike-slip terminal structures. New data, and the recognition that InSAR data will increasingly allow for the distinction between "visible" surface rupture lengths (*VSRL*) from field-mapping and "detectable" surface rupture lengths (*DSRL*), has prompted a recalculation of the Clark *et al.* (2014) relation between rupture length and magnitude for SCR earthquakes. The *VSRL*

regressions indicate that Australian SCR earthquakes tend to be longer for a given magnitude than elsewhere in the world (e.g. Wells & Coppersmith, 1994; Leonard, 2014).

The September M_W 5.3 Lake Muir earthquake was the ninth event documented to have produced surface rupture in Australia in historical times (**Figure 1, Table 1**). These ruptures are located exclusively in the Precambrian SCR rocks of central and western Australia, and none could have been identified and mapped using topographic signature prior to the historical event. A pattern is also emerging where 'one-off' ruptures, as evidenced by the historic surface-breaking earthquakes, are filling the spaces between mapped multi-event neotectonic scarps (cf. Clark, 2010; Clark *et al.*, 2012; Clark *et al.*, 2019). Despite such observations, patterns of migration in intraplate seismicity, particularly in Precambrian SCR crust, are yet to be fully understood (Stein & Liu, 2009; Liu *et al.*, 2011).

DATA SOURCES

Source parameters of the earthquakes were obtained from the Geoscience Australia catalogue https://earthquakes.ga.gov.au/ (last accessed 08.02.2019). The datafile and code written to regress the length versus magnitude data are obtainable from the Geoscience Australia Github repository https://github.com/GeoscienceAustralia/GA-neotectonics/tree/master/Lake_Muir_Solid_Earth_data. The precise orbital ephemerides products used in correcting the InSAR data are available from https://qc.sentinel1.eo.esa.int/aux_poeorb/.

ACKNOWLEDGEMENTS

Thanks to Roger Hearn of Manjimup for conducting the initial field reconnaissance and taking the first photos of the scarp. Thanks also to Rob De Campo and Mark Muir for providing access to their properties to conduct fieldwork. We acknowledge the Minang Noongar as the traditional owners of the land on which our field work took place. This manuscript is published with the permission of the CEO of Geoscience Australia.

REFERENCES

Allen, T., Carapetis, A., Bathgate, J., Ghasemi, H., Pejić, T. & Moseley, A. 2019a. Real-Time Community Internet Intensity Maps and ShakeMaps for Australian earthquakes. *Australian Earthquake Engineering Society 2019 Conference, Nov 29 – Dec 1, Newcastle, NSW.*

Allen, T., Clark, D., Lawrie, S., Brenn, G., Dimech, J., Garthwaite, M., Glanville, H., Kemp, T., Lintvelt, C., Lumley, D., Pejic, T., Sayin, E. & Standen, S. 2019b. The 2018 Lake Muir earthquakes: Australia's ninth surface rupturing earthquake sequence in 50 years. *Seismological Research Letters*, 90 951.

Allen, T.I., Dhu, T., Cummins, P.R. & Schneider, J.F. 2006. Empirical Attenuation of Ground-Motion Spectral Amplitudes in Southwestern Western Australia. *Bulletin of the Seismological Society of America*, 96: 572-585.

Allen, T.I., Leonard, M., Ghasemi, H. & Gibson, G. 2018. The 2018 National Seismic Hazard Assessment for Australia – earthquake epicentre catalogue. *Geoscience Australia Record* 2018/30, doi: 10.11636/Record.2018.030.

Allmann, B.P. & Shearer, P.M. 2009. Global variations of stress drop for moderate to large earthquakes. *Journal of Geophysical Research: Solid Earth*, 114(B1): B01310, 10.1029/2008jb005821.

Boncio, P., Liberi, F., Caldarella, M. & Nurminen, F.-C. 2018. Width of surface rupture zone for thrust earthquakes: implications for earthquake fault zoning. *Natural Hazards and Earth System Sciences*, 18: 241-256, https://doi.org/10.5194/nhess-18-241-2018.

Bowman, J.R. 1992. The 1988 Tennant Creek, Northern Territory, earthquakes: a synthesis. *Australian Journal of Earth Sciences*, 39(5): 651-669.

Braun, J., Burbidge, D., Gesto, F., Sandiford, M., Gleadow, A., Kohn, B. & Cummins, P. 2009. Constraints on the current rate of deformation and surface uplift of the Australian continent from a new seismic database and low-T thermochronological data. *Australian Journal of Earth Sciences*, 56: 99-110.

Brune, J.N. 1970. Tectonic stress and the spectra of seismic shear waves from earthquakes. *J. Geophys. Res.*, 75(26): 4997-5009.

Calais, E., Camelbeeck, T., Stein, S., Liu, M. & Craig, T.J. 2016. A New Paradigm for Large Earthquakes in Stable Continental Plate Interiors. *Geophysical Research Letters*, 10.1002/2016GL070815.

Calais, E., Mattioli, G., DeMets, C., Nocquet, J.M. & Stein, S. 2005. Tectonic strain in plate interiors? *Nature Geoscience*, 438: E9-E10.

Camacho, A., Vernon, R.H. & Fitzgerald, J.D. 1995. Large volumes of anhydrous pseudotachylyte in the Woodroffe Thrust, eastern Musgrave Ranges, Australia. *Journal of Structural Geology*, 17: 371- 383.

Clark, D. 2010. Identification of Quaternary scarps in southwest and central west Western Australia using DEM-based hill shading: application to seismic hazard assessment and neotectonics. *International Journal of Remote Sensing*, 31(23): 6297-6325.

Clark, D. 2012. *Neotectonic Features Database, Geoscience Australia*. In: G. Australia (Editor). http://pid.geoscience.gov.au/dataset/ga/74056, Canberra.

Clark, D. & Edwards, M. 2018. 50th anniversary of the 14th October 1968 MW 6.5 (MS 6.8) Meckering earthquake. Australian Earthquake Engineering Society Pre-conference Field Trip, Meckering, 15 November 2018. *Geoscience Australia Record*, 2018/39: 47.

Clark, D., McPherson, A., Allen, T. & De Kool, M. 2014. Co-seismic surface deformation relating to the March 23, 2012 MW 5.4 Ernabella (Pukatja) earthquake, central Australia: implications for cratonic fault scaling relations. *Bulletin of the Seismological Society of America*, 104(1): 24-39, doi: 10.1785/0120120361.

Clark, D., McPherson, A., Cupper, M., Collins, C.D.N. & Nelson, G. 2015. The Cadell Fault, southeastern Australia: a record of temporally clustered morphogenic seismicity in a low-strain intraplate region. In: A. Landgraf, S. Kuebler, E. Hintersburger and S. Stein (Editors),

Geological Society, London, Special Publication *Seismicity, Fault Rupture and Earthquake Hazards in Slowly Deforming Regions*.

Clark, D., McPherson, A., Pillans, B., White, D. & Macfarlane, D. 2017. Potential geologic sources of seismic hazard in Australia's south-eastern highlands: what do we know? *Australian Earthquake Engineering Society 2017 Conference, Nov 24-26, Canberra, ACT*: https://www.aees.org.au/wp-content/uploads/2018/02/420-Dan-Clark.pdf.

Clark, D., McPherson, A. & Van Dissen, R. 2012. Long-term behaviour of Australian Stable Continental Region (SCR) faults. *Tectonophysics* 566-567: 1-30, http://dx.doi.org/10.1016/j.tecto.2012.07.004.

Clark, D.J., Brennand, S., Brenn, G., Allen, T.I., Garthwaite, M.C. & Standen, S. 2019. The 2018 Lake Muir earthquake sequence, southwest Western Australia: rethinking Australian stable continental region earthquakes. *Solid Earth Discussion papers*, in review, https://doi.org/10.5194/se-2019-125.

Craig, T.J., Calais, E., Fleitout, L., Bollinger, L. & Scotti, O. 2016. Evidence for the release of long-term tectonic strain stored in continental interiors through intraplate earthquakes. *Geophysical Research Letters*, 43, doi:10.1002/2016GL069359.

Crone, A.J., Machette, M.N. & Bowman, J.R. 1992. Geologic investigations of the 1988 Tennant Creek, Australia, earthquakes - implications for paleoseismicity in stable continental regions. *United States Geological Survey Bulletin*, 2032-A: 51p.

Crone, A.J., Machette, M.N. & Bowman, J.R. 1997. Episodic nature of earthquake activity in stable continental regions revealed by palaeoseismicity studies of Australian and North American Quaternary faults. *Australian Journal of Earth Sciences*, 44: 203-214.

Dawson, J., Cummins, P., Tregoning, P. & Leonard, M. 2008. Shallow intraplate earthquakes in Western Australia observed by Interferometric Synthetic Aperture Radar. *Journal of Geophysical Research*, 113(B11408): doi:10.1029/2008JB005807.

Denham, D., Alexander, L.G., Everingham, I.B., Gregson, P.J., McCaffrey, R. & Enever, J.R. 1987. The 1979 Cadoux earthquake and intraplate stress in Western Australia. *Australian Journal of Earth Sciences*, 34(4): 507-521.

Denham, D., Alexander, L.G. & Worotnicki, G. 1980. The stress field near the sites of the Meckering (1968) and Calingiri (1970) earthquakes, Western Australia. *Tectonophysics*, 67: 283-317.

Dent, V.F. 2016. A preliminary map of cluster locations in southwest Western Australia, 1990 – 2016. *Joint Conference of the Australian Earthquake Engineering Society and the Asian Seismological Commission, Melbourne, Australia*, Paper 391.

Dentith, M.C., Dent, V.F. & Drummond, B.J. 2000. Deep crustal structure in the southwestern Yilgarn Craton, Western Australia. *Tectonophysics*, 325: 227-255.

Doyle, H.A. 1971. Seismicity and structure in Australia. *Bulletin of the Royal Society of New Zealand*, 9: 149-152.

Drummond, B.J., Goleby, B.R. & Swager, C.P. 2000. Crustal signature of Late Archaean tectonic episodes in the Yilgarn Craton, Western Australia: evidence from deep seismic sounding. *Tectonophysics*, 329: 193-221.

Gold, R.D., Clark, D., Barnhart, W.D., King, T., Quigley, M. & Briggs, R.W. 2019. Surface rupture and distributed deformation revealed by optical satellite imagery: The intraplate 2016 Mw 6.0 Petermann Ranges earthquake, Australia. *Geophysical Research Letters*, 46, https://doi.org/10.1029/2019GL084926.

Goleby, B.R., Shaw, R.D., Wright, C., Kennett, B.L.N. & Lambeck, K. 1989. Geophysical evidence for 'thick-skinned' crustal deformation in central Australia. *Nature*, 337: 325-330.

Gordon, F.R. & Lewis, J.D. 1980. The Meckering and Calingiri earthquakes October 1968 and March 1970. *Western Australia Geological Survey Bulletin*, 126: 229p.

Johnston, A.C., Coppersmith, K.J., Kanter, L.R. & Cornell, C.A. 1994. The earthquakes of stable continental regions. *Electric Power Research Institute Report.*, TR102261V1.

King, T., Quigley, M.C. & Clark, D. 2018. Surface effects produced by the Mw 6.1 20th May 2016 Petermann earthquake (Australia) and their use in Environmental Seismic Intensity evaluation. *Tectonophysics*, 747-748: 357-372.

Korsch, R.J., Goleby, B.R., Leven, J.H. & Drummond, B.J. 1998. Crustal architecture of central Australia based on deep seismic reflection profiling. *Tectonophysics*, 288: 57-69.

Leonard, M. 2002. The Burrakin WA earthquake sequence Sept 2000 - June 2002. *Australian Earthquake Engineering Society Conference - Total Risk Management in the Privatised Era*, Adelaide: Paper 22.

Leonard, M. 2008. One hundred years of earthquake recording in Australia. *Bulletin of the Seismological Society of America*, 98: 1458-1470.

Leonard, M. 2014. Self Consistent Earthquake Fault Scaling Relations: Update and Extension to Stable Continental Strike-Slip Faults. *Bulletin of the Seismological Society of America*, 104(6): 2953-2965.

Leonard, M., Burbidge, D.R., Allen, T.I., Robinson, D.J., McPherson, A., Clark, D. & Collins, C.D.N. 2014. The Challenges of Probabilistic Seismic Hazard Assessment in Stable Continental Interiors: An Australian Example *Bulletin of the Seismological Society of America* 104(6): 3008-3028, 10.1785/0120130248.

Leonard, M. & Clark, D. 2011. A record of stable continental region earthquakes from Western Australia spanning the late Pleistocene: Insights for contemporary seismicity. *Earth and Planetary Science Letters*, 309: 207-212.

Lewis, J.D., Daetwyler, N.A., Bunting, J.A. & Moncrieff, J.S. 1981. The Cadoux earthquake. *Western Australia, Geological Survey Report*, 1981/11: 133.

Liu, M. & Stein, S. 2016. Mid-continental earthquakes: Spatiotemporal occurrences, causes, and hazards. *Earth Science Reviews*, 10.1016/j.earscirev.2016.09.016.

Liu, M., Stein, S. & Wang, H. 2011. 2000 years of migrating earthquakes in North China: How earthquakes in midcontinents differ from those at plate boundaries. *Lithosphere*, doi: 10.1130/L129.1.

Machette, M.N., Crone, A.J. & Bowman, J.R. 1993. Geologic investigations of the 1986 Marryat Creek, Australia, earthquake - implications for paleoseismicity in stable continental regions. *USGS Bulletin*, 2032-B: 29 p.

Musson, R.M.W. 2012. Interpreting intraplate tectonics for seismic hazard: a UK historical perspective. *Journal of Seismology*, 16(2): 261-273, 10.1007/s10950-011-9268-1.

Okada, Y. 1985. Surface deformation due to shear and tensile faults in a half-space. *Bulletin of the Seismological Society of America*, 75(4): 1135-1154.

Polcari, M., Albano, M., Atzori, S., Bignami, C. & Stramondo, S. 2018. The Causative Fault of the 2016 Mwp 6.1 Petermann Ranges Intraplate Earthquake (Central Australia) Retrieved by C- and L-Band InSAR Data. *Remote Sensing*, 10: 1311, doi:10.3390/rs10081311.

Rajabi, M., Tingay, M., Heidbach, O., Hillis, R. & Reynolds, S. 2017. The present-day stress field of Australia. *Earth-Science Reviews*, 168: 165-189, 10.1016/j.earscirev.2017.04.003.

Stein, S. & Liu, M. 2009. Long aftershock sequences within continents and implications for earthquake hazard assessment. *Nature*, 462: 87-89.

Tregoning, P. 2003. Is the Australian Plate deforming? A space geodetic perspective. *Geolical Society of Australia Special Publication, 22 and Geological Society of America Special Publication, 372*: 41-48.

Wang, S., Xu, W., Xu, C., Yin, Z., Burgmann, R., Liu, L. & Jiang, G. 2019. Changes in Groundwater Level Possibly Encourage Shallow Earthquakes in Central Australia: The 2016 Petermann Ranges Earthquake. *Geophysical Research Letters*, 46, https://doi.org/10.1029/2018GL080510.

Wells, D.L. & Coppersmith, K.J. 1994. New empirical relationships among magnitude, rupture length, rupture width, rupture area, and surface displacement. *Bulletin of the Seismological Society of America*, 84(4): 974-1002.